Effect of Mean Stress Dependency of Elastic Soil Moduli on the Constitutive Behavior of Sand through UBCSAND

E. Tatlioglu[1], M. B. C. Ulker[2], M. A. Lav[1]

[1] **Department of Civil Engineering, Istanbul Technical University, Istanbul, Turkey**

[2] **Institute of Earthquake Engineering and Disaster Management, Istanbul Technical University, Istanbul, Turkey**

1 Abstract

In this study, nonlinear elastic behavior of sandy soils is studied with a UBCSAND constitutive model under static conditions. UBCSAND is an elastic-plastic soil model used in advanced stress deformation analyses of geotechnical systems. Not only the model predicts the static failure loads fairly accurately, it is also capable of capturing the excess pore water pressure accumulation leading to liquefaction of loose sands under cyclic loads. For that, a number of drained and undrained triaxial shear tests are simulated based upon the UBCSAND model considering various approaches of handling nonlinear elasticity. Mathematical formulation of the model is developed using the theory of classical plasticity and the elastoplastic tangent constitutive matrix is derived. The integration of the constitutive equations is performed through a fully explicit scheme and state variables are updated for each strain increment at the Gauss points. In the model, soil behavior is constituted as non-linear elastoplastic where the stress-dependent elastic bulk and shear moduli are utilized to govern the elastic behavior. As per the main objective of this study, various approaches of calculating the elastic component of the soil behavior by employing nonlinear variation of elastic soil moduli with the mean effective stress are presented. The predicting capabilities of these methods are discussed in terms of stress-strain relationship as well as stress path behaviors of various sands. The results show that the UBCSAND model can effectively and, to some extent, accurately capture the static behavior of sands over a wide range of drainage conditions provided that the elastic shear and bulk moduli are mostly dependent upon the mean effective stress.

2 Introduction

Constitutive modeling in soil mechanics is important in terms of understanding the real behavior of soils under design loads. There is a variety of theoretical models developed since the early era of geotechnical engineering dating back to the late

19th century. Among the relatively recent ones, the model proposed by the University of British Columbia that captures, to a certain degree, the static and dynamic behavior of sands, namely UBCSAND, is a considerably powerful one. This model is first developed in two-dimensional (2-D) stress state formulation by Puebla et al. (1997) and later extended by Beaty and Byrne (1998). Tsegaye (2010) expanded the model to its 3-D formulation. Then, Petalas and Galavi (2012, 2013) improved the model by adding a soil densification rule in order to predict more realistic evolution of excess pore pressure during cyclic response.

Given the initial elastic response, post-yield behavior of soils are significantly influenced by the elastic components of the stress-strain relationship. Generally speaking, the main source of the stress-strain response is associated with material plasticity as soils are highly deformable materials exhibiting irrecoverable strains. Since the tangent stiffness matrix of soils has both elastic and plastic parts, the overall behavior throughout any course of loading essentially includes both components. That said, elastic properties of soils which depend upon drainage conditions and internal stress directions, are hence mostly not constant in the field. . In fact, some of the truly elastic properties of soils vary with the effective stress level which is the actual source of elastic nonlinearity (Wood, 2004; Poorooshasb and Yang, 1990). Such a behavior can be attributed to the fact that soils are ultimately pressure dependent materials and there is a wide range of existing empirical relations for pressure-dependent stiffness of soils (Einav et. al, 2004).

In this study, our main focus is on the static behavior of sandy soils. For that, a number of drained and undrained triaxial shear tests are simulated through the UBCSAND model. Firstly, theoretical results are verified with the results of a set of preliminary strain-controlled triaxial tests. Here, volumetric strains as well as pore pressure generations are evaluated in drained and undrained tests, respectively. Subsequently, a partial drainage condition is also defined using a strain ratio and such an intermediate case where both response results are obtained, is simulated.

3 Constitutive Model

The formulation of the original UBCSAND model is based on classical plasticity. Model uses a Mohr-Coulomb type yield function and a hyperbolic strain hardening law along with a non-associated flow rule. Hardening law relates the mobilized friction angle to plastic shear strain increments at a given stress level. In the model, soil behavior is considered elastoplastic where the elastic moduli are taken as effective stress-dependent. The modified version of the UBCSAND model uses a Mohr-Coulomb yield criterion in a 3-D principal stress space and a modified plastic potential function based on the Drucker-Prager´s criterion (Tsegaye 2010). Plasticity components of the model are given below.

3.1 Yield Surface

UBCSAND model uses the well-known Mohr-Coulomb yield function generalized in 3-D principal stress space given as;

$$f_m = \frac{\sigma'_{\max} - \sigma'_{\min}}{2} - \left(\frac{\sigma'_{\max} + \sigma'_{\min}}{2} + c' \cot \phi'_p\right) * \sin \phi_m \quad (1)$$

where $\sigma'_{\max}$ and $\sigma'_{\min}$ are the maximum and minimum effective stresses, c' is the cohesion of the soil, ϕ_p is the peak friction angle and ϕ_m is the mobilized friction angle during hardening.

3.2 Elastic Behavior

The elastic behavior within the yield surface is governed by a non-linear rule as a function of mean effective stress. Elastic bulk modulus K_0^e and elastic shear modulus G_0^e are the initial parameters used to simulate the non-linear elastic behavior. The proposed methods governing the elastic component of the entire elastoplastic response of sand which is the main objective of this study are given in details in section 5.

3.3 Elasto-Plastic Behavior

According to Beaty and Byrne (1998), the deviatoric hardening law relates the increment of the sine of the mobilized friction angle to the plastic shear strain increment. The mobilized friction angle is given as:

$$\sin \varphi_m = \frac{q_m}{p_m} \quad (2)$$

where

$$q_m = \frac{\sigma'_{\max} - \sigma'_{\min}}{2} \qquad p_m = \frac{\sigma'_{\max} + \sigma'_{\min}}{2} \quad (3)$$

are the stress state parameters. Hardening law can be written as (Tsegaye, 2010):

$$d\sin\phi_m = k_G^p \left(\frac{p_m}{p_A}\right)^{np-1} \left(1 - \frac{\sin\phi_m}{\sin\phi_p} * R_f\right)^2 d\varepsilon_q^p \quad (4)$$

where k_G^p is the plastic shear modulus number, np is the model parameter, p_A is the atmospheric pressure and R_f is the failure ratio. Plastic potential function is defined by Puebla (1997) as:

$$g_m = q_m - \sin\psi \left(p_m + c \cot \varphi_p\right) \quad (5)$$

where

$$\sin\psi = \sin\varphi_m - \sin\varphi_{cv} \tag{6}$$

Here ϕ_{cv} is the critical friction angle. The non-associated flow rule is given within the context of stress-strain relationship below.

3.4 Stress-Strain Relationship

The strain decomposition in an incremental form is written as,

$$d\underset{\sim}{\varepsilon} = d\underset{\sim}{\varepsilon}^e + d\underset{\sim}{\varepsilon}^p \tag{7}$$

where $d\varepsilon^e$ is elastic and $d\varepsilon^p$ is the plastic strain increment. Taking the elastic strains from this relation and using in the stress-strain relationship, we get:

$$d\underset{\sim}{\sigma} = \underset{\sim}{D}^e(d\underset{\sim}{\varepsilon} - d\underset{\sim}{\varepsilon}^p) \tag{8}$$

where D^e is the elastic constitutive matrix and stress increment is defined as $d\underset{\sim}{\sigma} = \begin{pmatrix} dp_m \\ dq_m \end{pmatrix}$ in this study. Flow rule (non-associated form) is:

$$d\underset{\sim}{\varepsilon}^p = d\lambda \frac{\partial g}{\partial \underset{\sim}{\sigma}} \tag{9}$$

which, when used with (8), yields:

$$d\underset{\sim}{\sigma} = \underset{\sim}{D}^e(d\underset{\sim}{\varepsilon} - d\lambda \frac{\partial g}{\partial \underset{\sim}{\sigma}}) \tag{10}$$

where $d\lambda$ is the plastic multiplier. Using the consistency condition including the hardening term we get:

$$\left(\frac{\partial f}{\partial \underset{\sim}{\sigma}}\right)^T d\underset{\sim}{\sigma} + d\lambda \frac{\partial f}{\partial sin\phi_m} . \frac{\partial sin\phi_m}{\partial \varepsilon^p_{qm}} \frac{\partial g}{\partial q_m} = 0 \tag{11}$$

If we substitute (10) into (11) below is obtained,

$$\left(\frac{\partial f}{\partial \underset{\sim}{\sigma}}\right)^T \underset{\sim}{D}^e(d\underset{\sim}{\varepsilon} - d\lambda \frac{\partial g}{\partial \underset{\sim}{\sigma}}) + d\lambda \frac{\partial f}{\partial sin\phi_m} . \frac{\partial sin\phi_m}{\partial \varepsilon^p_{qm}} \frac{\partial g}{\partial q_m} = 0 \tag{12}$$

which is now solved for $d\lambda$ as,

$$d\lambda = \frac{\left(\frac{\partial f}{\partial \underset{\sim}{\sigma}}\right)^T \underset{\sim}{D}^e d\underset{\sim}{\varepsilon}}{\left(\frac{\partial f}{\partial \underset{\sim}{\sigma}}\right)^T \underset{\sim}{D}^e \frac{\partial g}{\partial \underset{\sim}{\sigma}} - \frac{\partial f}{\partial sin\phi_m} . \frac{\partial sin\phi_m}{\partial \varepsilon^p_{qm}} \frac{\partial g}{\partial q_m}} \tag{13}$$

where the plastic modulus is:

$$H = -\frac{\partial f}{\partial \sin\phi_m}\frac{\partial \sin\phi_m}{\partial \varepsilon_{qm}^{p}}\frac{\partial g}{\partial q_m} \tag{14}$$

Final stress-strain relationship in incremental form becomes,

$$d\underset{\sim}{\sigma} = \underset{\approx}{D}^{e}\left(I - \frac{\frac{\partial g}{\partial \underset{\sim}{\sigma}}\left(\frac{\partial f}{\partial \underset{\sim}{\sigma}}\right)^{T}\underset{\approx}{D}^{e}}{\left(\frac{\partial f}{\partial \underset{\sim}{\sigma}}\right)^{T}\underset{\approx}{D}^{e}\frac{\partial g}{\partial \underset{\sim}{\sigma}} + H} \right) d\underset{\sim}{\varepsilon} \tag{15}$$

where the tangent elasto-plastic constitutive matrix $\underset{\approx}{D}^{ep}$ is:

$$\underset{\approx}{D}^{ep} = \underset{\approx}{D}^{e} - \frac{\underset{\approx}{D}^{e}\frac{\partial g}{\partial \underset{\sim}{\sigma}}\left(\frac{\partial f}{\partial \underset{\sim}{\sigma}}\right)^{T}\underset{\approx}{D}^{e}}{\left(\frac{\partial f}{\partial \underset{\sim}{\sigma}}\right)^{T}\underset{\approx}{D}^{e}\frac{\partial g}{\partial \underset{\sim}{\sigma}} + H} \tag{16}$$

4 Verification of the Static Behavior

To demonstrate the accuracy of the simulation, model predictions are compared with the experimental results and fairly acceptable agreements are achieved between the results (Fig. 1-2). The analyses are performed using a fully explicit integration method through the forward Euler scheme.

Fig. 1 shows the comparison of the triaxial tests (Eliadorani, 2000) and the simulation results. Comparisons are obtained in terms of shear stress-axial strain relations and stress path plots in Fig.1for fully undrained and partially drained tests. Partial drainage condition is defined as:

$$d\varepsilon_p = -d\varepsilon_1 \tag{17}$$

where $d\varepsilon_p$ is the volumetric strain. Fig. 2 presents the results for the fully drained condition. The tests are obtained from Tsegaye, (2010).

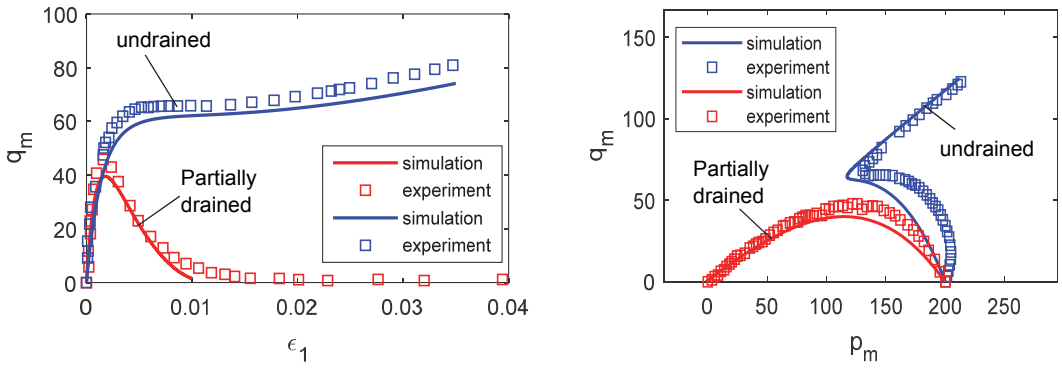

Fig. 1: Simulation of undrained and partially drained triaxial test

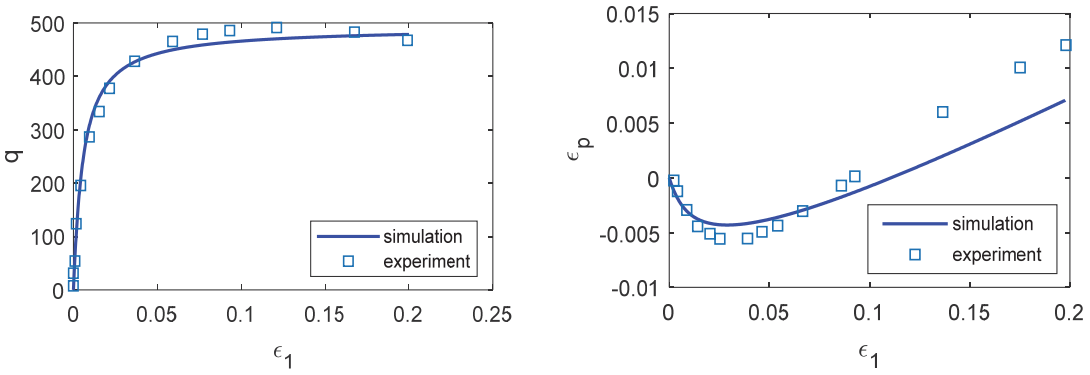

Fig. 2: Simulation of drained triaxial test

5 Nonlinear Elastic Behavior

A total of five different methods for calculating the elastic shear and bulk moduli are presented in Tab.1. Except for the first method which keeps the moduli constant, the rest of the methods consider the stress-dependence of the moduli nonlinear (Methods 2 and 3) and linear (Methods 4 and 5). Method 3 uses nonlinear elastic behavior of the UBCSAND model as given by Puebla (1997). Method 2 relies on a fit parameter 'α' linking the shear and bulk moduli. Method 3, although an independent method by itself, can be converted to Method 2 provided that the α constant is a function of the Poisson's ratio. Method 5 is a linear function of the mean stress with an A_0 coefficient as used by Poorooshasb et al. (1990). The comparison results are shown in Fig.3-7 for all methods under the three drainage conditions of fully drained, fully undrained and an intermediate partially drained cases.

Tab. 1: Equations of shear and bulk modulus

Method	Shear modulus relations	Bulk modulus relations
1	$G^e = G_0^e$	$K^e = K_0^e$
2	$G^e = G_0^e . \left(\frac{p'}{p_A} \right)^{ne}$	$K^e = \alpha . G^e$
3	$G^e = G_0^e . \left(\frac{p'}{p_A} \right)^{ne}$	$K^e = K_0^e . \left(\frac{p'}{p_A} \right)^{me}$ or $K^e = \alpha . G^e$ with $\alpha = \frac{2(1+\nu)}{3(1-2\nu)}$
4	$G^e = G_0^e . \frac{p'}{p_A}$	$K^e = K_0^e . \frac{p'}{p_A}$
5	$G^e = G_0^e + A_0 . \frac{G_0^e}{K_0^e} p'$	$K^e = K_0^e + A_0 p'$

Test data and model parameters are taken from Tsegaye (2010) for obtaining Figs. 3 and 5. Other tests are obtained from Eliadorani (2000) and their respective model parameters from Atigh (2004). Even though Methods 1 and 2 seem to yield similar results in the undrained and partially drained tests considered in this study, we can say for all comparisons that Method 2 governs the nonlinear elastic behavior of sandy soils more accurately than others.

- **Drained Triaxial Test Simulations**

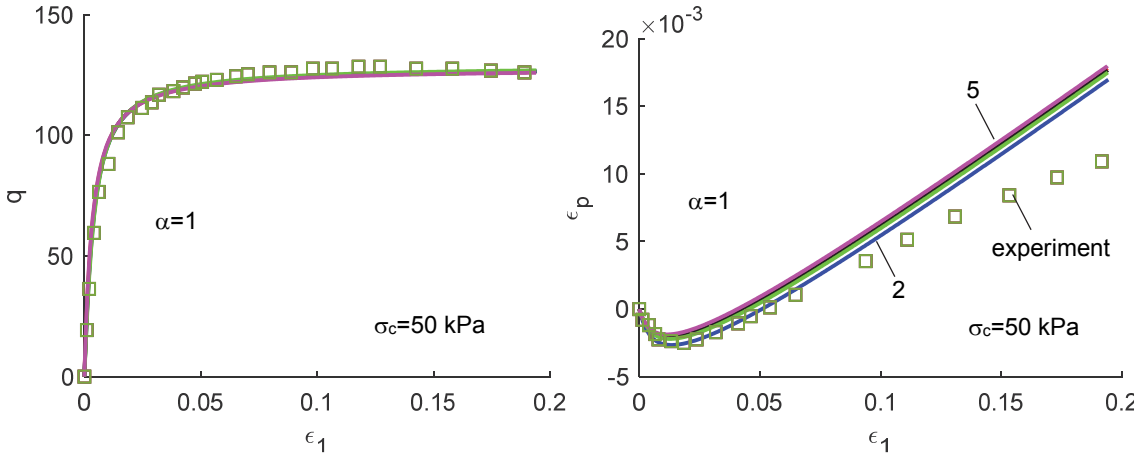

Fig. 3: Comparison of nonlinear elastic behavior with different methods under drained condition a) $q-\varepsilon_1$ b) $\varepsilon_p-\varepsilon_1$

According to Fig.3, all methods yield similar stress-strain behaviors under low consolidation pressures. Values of shear and bulk moduli tend to become constant due to the increase in mean effective stress during the test. This may be the reason for obtaining the similar behavior between different methods for the drained tests. On the other hand, differences between the methods can be seen under high consolidation pressures at small strain levels (Fig.4). Method 2 simulates the volumetric deformation better than others in Fig.4b.

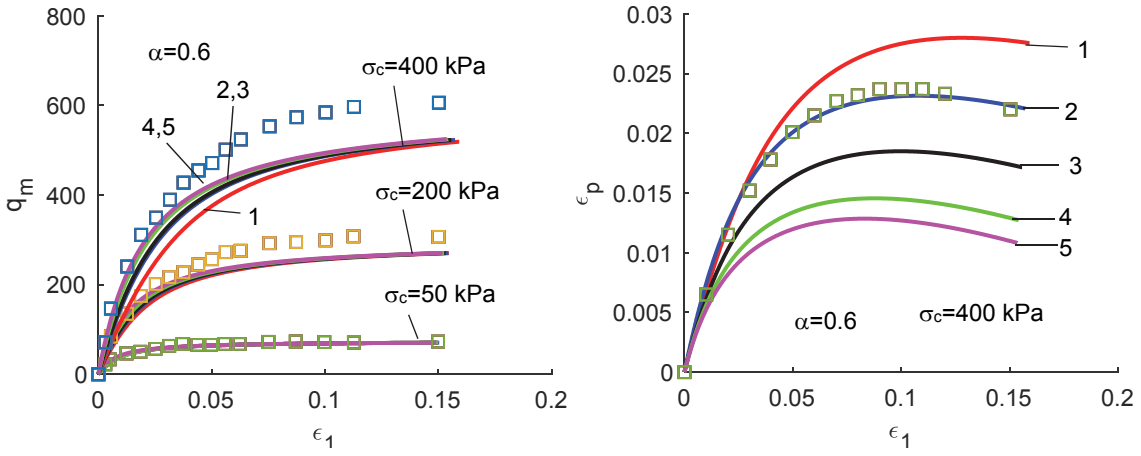

Fig. 4: Comparison of nonlinear elastic behavior with different methods under drained condition a) $q_m-\varepsilon_1$ b) $\varepsilon_p-\varepsilon_1$

- **Undrained Triaxial Test Simulations**

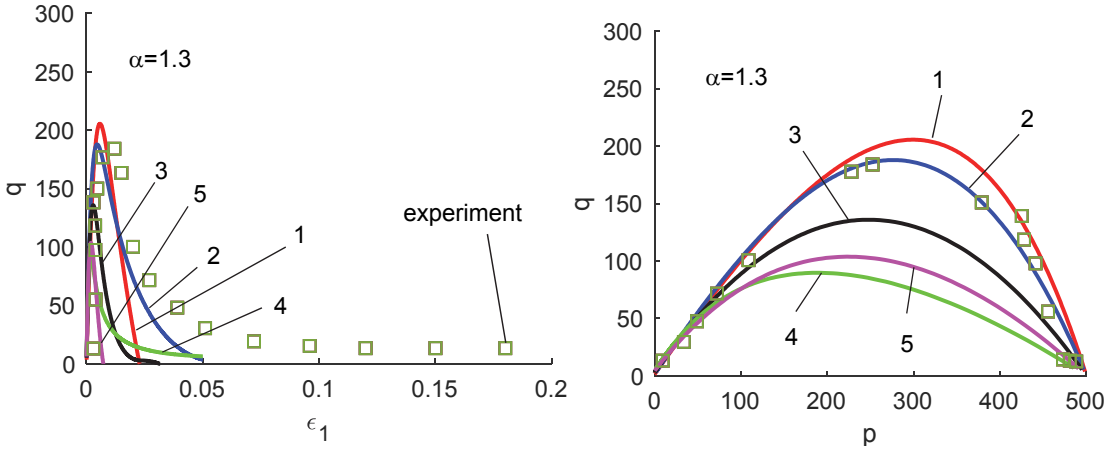

Fig. 5: Comparison of nonlinear elastic behavior with different methods under undrained condition a) $q-\varepsilon_1$ b) $q-p$

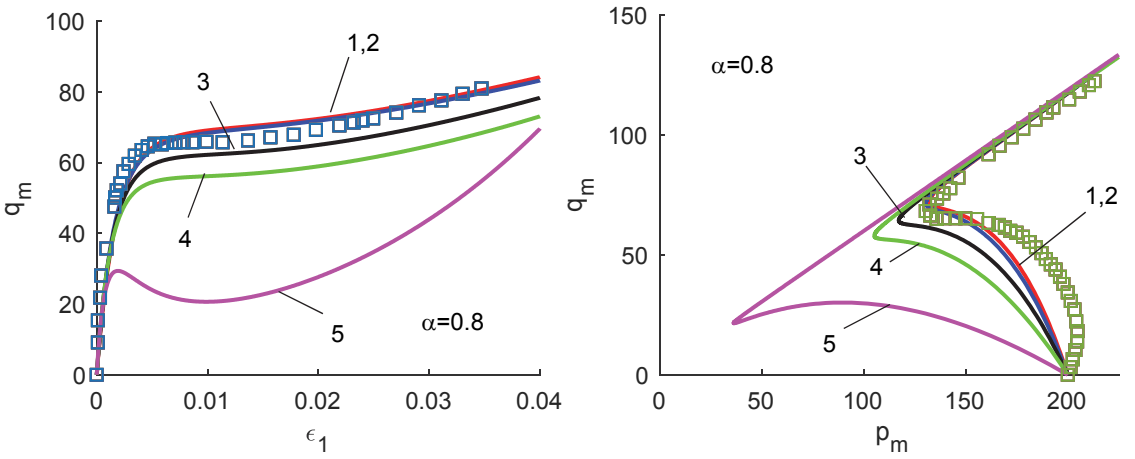

Fig. 6: Comparison of nonlinear elastic behavior with different methods under undrained condition a) $q_m-\varepsilon_1$ b) q_m-p_m

For the undrained triaxial test simulations (Figs.5-6), Method 1 and Method 2 yield in overall better comparisons with the experimental results. It should, however, be noted here that Method 1 is stress-independent and basically assumes constant elastic moduli. That is as if to mention that, as the elastic relationship of the moduli are independent of the mean stress level in the soil, the response is captured more accurately. However, we tend to discard this seemingly misleading outcome based on the number of test data available as well as the number of analyses we have made in this study. Therefore, we consider Method 2 as the most appropriate one to capture the undrained response. This can also be seen in Fig.7a where not only the peak shear response is predicted well but the residual response is captured fairly accurately also by the Method 2.

- **Partially Drained Triaxial Test Simulations**

The results presented in most of the analyses show that Method 5 does not have the capability to explain the nonlinear elastic behavior of sands during an elastoplastic loading. This may be due to the reliability of the method on the A_0 coefficient whose possible dependence on the physical parameters of sand is unknown a-priori (Poorooshasb and Yang, 1990). It can also be observed that Methods 3 and 4 lack a good agreement with that of the related experiments, Method 3 giving better results than Method 4.

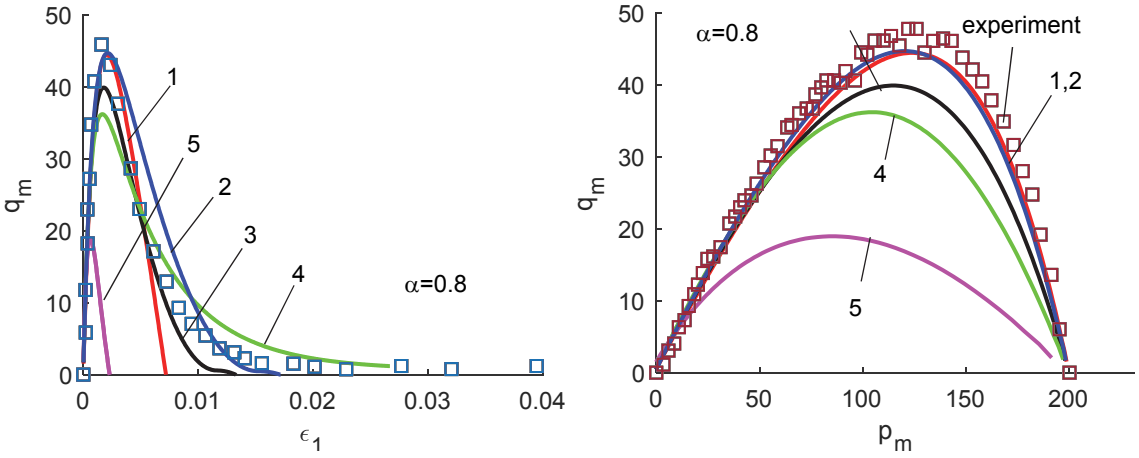

Fig. 7: Comparison of nonlinear elastic behavior with different methods under partial drainage condition a) $q_m - \varepsilon_1$ b) $q_m - p_m$

6 Conclusions

The main conclusions obtained in this study are the following:

- UBCSAND model is capable of capturing the the static response of sands fairly accurately under various confining pressures.
- Elastic shear and bulk moduli are highly dependent upon the mean effective stress. Such dependence affects the elastoplastic response of sands for a variety of drainage conditions.
- Method 2 provides the most predicting capacity with the given test results to simulate the nonlinear elastic behavior of sandy soils in terms of elastic moduli.

7 References

Atigh, E. & Byrne, P.M. (2004)
Liquefaction flow of submarine slopes under partially undrained conditions: an effective stress approach. Can. Geotech. J. 41: 154–165.

Beaty, M. H. & Byrne, P. (1998)
An Effective Stress for Predicting Liquefaction Behavior of Sand. Geotechnical Earthquake Eng. and Soil Dynamics III, Geotechnical Sp. Pub., 1, 766–777.

Eliadorani, A.A. (2000).
The response of sands under partially drained states with emphasis on liquefaction. Ph.D. thesis, The University of British Columbia, Vancouver.

Einav, I. and Alexander, M. Puzrin, ASCE, A.M. (2004).
Pressure-Dependent Elasticity and Energy Conservation in Elastoplastic Models for Soils, J. of Geotech. and Geoenvironmental Eng., 130(1):81-92.

Petalas, A., V. Galavi, and R.B.J. Bringkreve. (2012).
Validation and verification of a practical constitutive model for predicting liquefaction in sands. Pro-ceedings of the 22nd european young geotechnical engineers conference, Gothenburg, Sweden., pages 167-172.

Petalas, A., and Galavi, V. (2013).
Plaxis Liquefaction Model UBC3D-PLM.

Poorooshasb HB and Yang QS, Clark JI. (1990).
Non-linear analysis of a seabed deposit subjected to the action of standing waves. Math. Comp. Model, 13(4):45-58.

Puebla, H., Byrne, P. M., and Phillips, R. (1997).
Analysis of CANLEX liquefaction embankments: prototype and centrifuge models.” Can. Geotech J., 34(5), 641–657.

Tsegaye, A. B. (2010).
Liqueafaction model (UBC3D), Technical Report, Plaxis B.V., Delft.

Wood, D.M. (2004).
Geotechnical Modelling, Version 2.2, April.